Boron oxides under pressure: Prediction of the hardest oxides

Huafeng Dong,[1] Artem R. Oganov,[2,*] Vadim V. Brazhkin,[3] Qinggao Wang,[4] Jin Zhang,[5] M. Mahdi Davari Esfahani,[5] Xiang-Feng Zhou,[6] Fugen Wu,[1] and Qiang Zhu[7]

[1]*School of Physics and Optoelectronic Engineering, Guangdong University of Technology, Guangzhou 510006, China*
[2]*Skolkovo Institute of Science and Technology, Skolkovo Innovation Center, 3 Nobel Street, Moscow 143026, Russia; Moscow Institute of Physics and Technology, 9 Institutskiy Lane, Dolgoprudny City, Moscow Region 141700, Russian Federation; and International Center for Materials Discovery, Northwestern Polytechnical University, Xi'an 710072, China*
[3]*Institute for High Pressure Physics, Russian Academy of Sciences, Troitsk, Moscow, 108840 Russia*
[4]*Institute for Computational Materials Science, School of Physics and Electronics, Henan University, Kaifeng 475004, China*
[5]*Department of Geosciences and Center for Materials by Design, Institute for Advanced Computational Science, State University of New York, Stony Brook, New York 11794, USA*
[6]*School of Physics and Key Laboratory of Weak-Light Nonlinear Photonics, Nankai University, Tianjin 300071, China*
[7]*Department of Physics and Astronomy, High Pressure Science and Engineering Center, University of Nevada, Las Vegas, Nevada 89154-4002, USA*

(Received 4 August 2017; revised manuscript received 5 September 2018; published 21 November 2018)

We search for stable compounds of boron and oxygen at pressures from 0 to 500 GPa using the *ab initio* evolutionary algorithm USPEX. Only two stable stoichiometries of boron oxides, namely, B_6O and B_2O_3, are found to be stable, in good agreement with experiment. A hitherto unknown phase of B_6O at ambient pressure, $Cmcm$-B_6O, has recently been predicted by us and observed experimentally. For B_2O_3, we predict three previously unknown stable high-pressure phases—two of these ($Cmc2_1$ and $P2_12_12_1$) are dynamically and mechanically stable at ambient pressure, and should be quenchable to ambient conditions. Their predicted hardnesses, reaching 33–35 GPa, make them harder than SiO_2-stishovite. These are the hardest known oxides (if one disregards B_6O, which is essentially a boron-based insertion compound). Under pressure, the coordination number of boron atoms changes from 3 to 4 to 6, skipping fivefold coordination.

DOI: 10.1103/PhysRevB.98.174109

I. INTRODUCTION

Boron (B) is arguably the most complicated element in the Periodic Table, with as many as 16 allotropes experimentally reported, most of which are probably impurity-stabilized. Well-established α, β, γ, and tetragonal T allotropes are superhard, and have been confirmed to be pure boron allotropes [1]. Recently, yet another pure bulk modification of boron, τ-B [2], and two-dimensional (2D) allotropes of boron, borophenes, were identified [3,4]. Boron oxide B_2O_3 and suboxide B_6O are well established, but there are also controversial compounds proposed in the literature [4–15].

To date, two crystalline forms of B_2O_3 are known: B_2O_3-I [5] (ambient-pressure form) and B_2O_3-II [6] (high-pressure form). B_2O_3-I is composed of BO_3 planar triangular units, while B_2O_3-II is made of BO_4 tetrahedra. The change of coordination number from 3 to 4 is similar to the structural transformation in the B_2O_3 glass under pressure [7]. However, the coordination number change in B_2O_3 glass under pressure is not without controversy [8–10]. Brazhkin *et al.* [8] observed the transformation of $^{[3]}B \rightarrow {}^{[4]}B$ (the superscript is the coordination number) by x-ray diffraction in B_2O_3 glass under pressure, and predicted one more transformation to $^{[6]}B$ using first-principles simulations at high pressure. Only four months later, Trachenko *et al.* [9] reported the transformation $BO_3 \rightarrow BO_4 \rightarrow BO_5 \rightarrow BO_6$ for the local coordination environments in B_2O_3 glass under pressure; and a similar trend was also observed by Vegiri and Kamitsos [10] in 0.3LiO-B_2O_3 glass.

Boron suboxides, such as B_2O [11], B_6O [12], $B_{13}O_2$ [13], B_7O [14], and $B_{22}O$ [15], have been reported and, if confirmed, could be promising superhard materials. Among these, B_2O (though studied by some theorists [16]), had already been ruled out [17]. B_6O, $B_{13}O_2$, B_7O, and $B_{22}O$ can be considered as insertion phases based on rhombohedral α-boron structure with icosahedral B_{12} units and interstitial oxygens. B_6O is the most extensively studied phase among them, and it was synthesized at ambient pressure [18], as opposed to diamond [19] and cubic BN [20], which are synthesized at high pressure. Given the numerous controversies in the literature, we decided to perform a thorough study of the structures and stability of B-O compounds at normal and high-pressure conditions by employing a systematic and unbiased first-principles crystal structure and compound prediction method.

II. METHOD OF CALCULATION

We used the *ab initio* evolutionary algorithm USPEX [21–23], which can simultaneously find the stoichiometry and crystal structures of all stable compounds in a multicomponent system. In our searches at each pressure point, the initial population included 120 structures with up to 32 atoms per primitive cell, with all subsequent generations consisting of 50 structures produced by heredity (30%), transmutation (20%),

*a.oganov@skoltech.ru

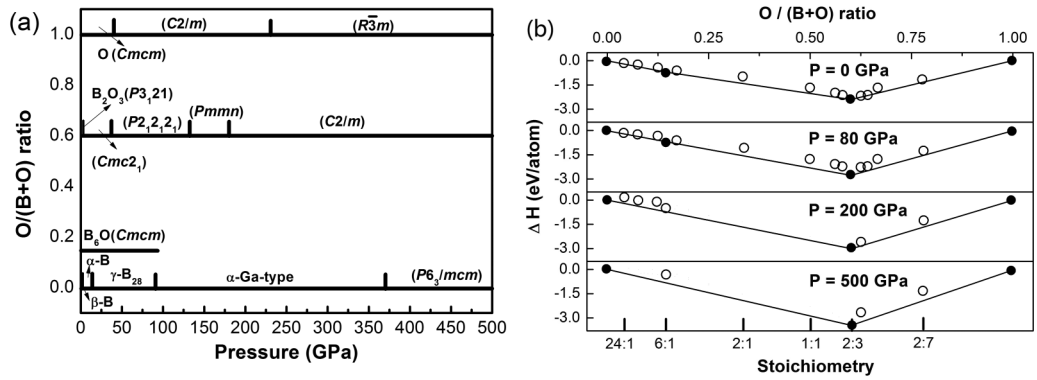

FIG. 1. Thermodynamic stability of boron oxides. (a) Pressure-composition phase diagram of the B-O system. (b) Thermodynamic convex hulls of the B-O system at selected pressures. Filled circles represent stable compounds; open circles denote metastable compounds. ΔH is the enthalpy of formation per atom (for details of the calculation process, see the Supplemental Material [31]).

softmutation (20%), and random symmetric generator (30%). Structure relaxations and total energy calculations were done within the generalized gradient approximation (GGA) [24] as implemented in the VASP [25] code. We used the PAW [26] method to represent core electrons and their effect on valence electrons, and the kinetic energy cutoff for valence wave functions was set to 600 eV, which gives excellent convergence of energy differences and stress tensors. Brillouin zone sampling was done with uniform Γ-centered k meshes with the resolution $2\pi \times 0.06\,\text{Å}^{-1}$ within USPEX searches and $2\pi \times 0.04\,\text{Å}^{-1}$ for further calculations of physical properties. Phonon dispersions were calculated using the finite-displacement method as implemented in the PHONOPY [27] code. Hardness was estimated using the empirical Chen-Niu [28] and Lyakhov-Oganov models [29]. At pressures below 5 GPa we included the van der Waals correction using the DFT-D2 method of Grimme [30].

III. RESULTS AND DISCUSSION

Variable-composition calculations were performed at pressures of 0, 20, 50, 100, 150, 200, 300, 400, and 500 GPa. We found that compositions B_2O_3, $B_{13}O_2$, BO, B_2O, B_6O, $B_{12}O$, and $B_{24}O$, are stable or close to the convex hull, which can be compared with the reported compositions, such as B_2O_3 [7], $B_{13}O_2$ [11], B_2O [11], B_4O [15], B_6O [18], B_7O [14], B_8O [15], $B_{10}O$ [15], and $B_{22}O$ [15]. For all the found and reported compositions, we carried out fixed-composition evolutionary searches at 0, 20, 40, 60, 80, 100, 150, 200, 250, 300, 350, 400, 450, and 500 GPa (up to 37 atoms per cell) to find the most stable structures. After this, the final pressure-composition phase diagram and convex hulls of the B-O system were constructed (see Fig. 1).

As can be seen from Fig. 1(b) and Fig. S1 in the Supplemental Material [31], B_2O, B_4O, B_7O, $B_{11}O$, $B_{12}O$, and $B_{24}O_3$ have enthalpies of formation near (though slightly above) the convex hull. Only B_2O_3 and B_6O lie on the convex hull, indicating stability of only these two compounds, which is in good agreement with the vast majority of experimental results [32,33]. B_6O is stable below 94 GPa; at higher pressures, B_2O_3 remains the only stable boron oxide (see Fig. 1).

Surprisingly, $Cmcm$-B_6O, rather than the well-known $R\bar{3}m$-B_6O (Fig. 2) [18], is found to be the stable phase of B_6O in the whole pressure range of 0–94 GPa; see Figs. 1(a) and Fig. S2 in the Supplemental Material online [31]). The enthalpy difference between these two structures is small (at ambient pressure it is only 1.8 meV per formula unit, and increases slightly with pressure). This prediction was published [12] and then our predicted $Cmcm$-B_6O phase was experimentally confirmed [34].

Below we focus on B_2O_3. We found the following sequence of pressure-induced phase transitions:

$$P3_121\text{-}B_2O_3(\text{I}) \overset{0.5}{\rightarrow} Cmc2_1\text{-}B_2O_3(\text{II}) \overset{46}{\rightarrow} P2_12_12_1\text{-}B_2O_3 \overset{133}{\rightarrow} Pmmn\text{-}B_2O_3 \overset{179}{\rightarrow} C2/m\text{-}B_2O_3.$$

The numbers above the arrows indicate the calculated phase transition pressures in GPa (Table I), at zero Kelvin.

At pressures below 0.5 GPa, B_2O_3 is stable in the $P3_121$ structure (this is the well-known B_2O_3-I phase). B_2O_3-I is composed of corner-sharing triangular BO_3 units; this ultraflexible [36] structure is shown in Fig. 3(a). From 0.5 to 46 GPa, $Cmc2_1$-B_2O_3, i.e., B_2O_3-II [6], is stable. B_2O_3-II is composed of BO_4 tetrahedra, as shown in Fig. 3(b). The $BO_3 \rightarrow BO_4$ coordination number change also occurs in the vitreous B_2O_3 under pressure. The transition pressure point, 0.5 GPa, is consistent with experiments on glassy B_2O_3 [37]

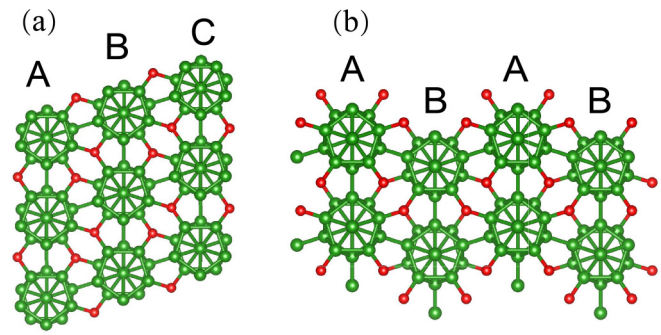

FIG. 2. Crystal structures of (a) $R\bar{3}m$-B_6O, (b) $Cmcm$-B_6O. Green (large) and red (small) spheres denote B and O atoms, respectively.

TABLE I. Crystal structures of experimentally known and recently predicted phases of B_6O and B_2O_3.

Phase	Pressure (GPa)	Volume (Å^3/atom)	Cell parameters	Atomic coordinates
$R\bar{3}m$-B_6O (expt. [18])	0	7.376	$a = 5.390$ Å $c = 12.313$ Å	N/A
$R\bar{3}m$-B_6O	0	7.387	$a = 5.393$ Å $c = 12.318$ Å	B1(0.110,0.221, 0.887); B2(0.317,0.158, 0.360) O(0.0,0.0, 0.622)
$Cmcm$-B_6O	0	7.384	$a = 5.393$ Å $b = 8.777$ Å $c = 8.736$ Å	B1 (0.0,0.756, 0.588); B2 (0.0,0.549, 0.584) B3 (0.165,0.824,0.750); B4 (0.238,0.155,0.649) B5 (0.334,0.987,0.750); O (0.0,0.840,0.439)
B_2O_3-I $P3_121$ (expt. [35])	0	9.053	$a = b = 4.336$ Å, $c = 8.340$ Å	B1 (0.395,0.230, 0.224); O1 (0.601,0.148,0.128); O2 (0.161, 0.0, 0.333)
$P3_121$-B_2O_3	0	9.007	$a = b = 4.348$ Å, $c = 8.251$ Å	B1 (0.395,0.236,0.225); O1(0.602,0.154,0.128); O2 (0.151, 0.0, 0.333)
B_2O_3-II $Cmc2_1$ (expt. [6])		7.432	$a = 4.613$ Å, $b = 7.803$ Å, $c = 4.129$ Å	B1 (0.161,0.165, 0.434); O1(0.370,0.291,0.580); O2 (0.248, 0.0, 0.5)
$Cmc2_1$-B_2O_3	0.5	7.462	$a = 4.608$ Å, $b = 7.808$ Å, $c = 4.149$ Å	B1 (0.161,0.164,0.433); O1(0.368,0.294,0.580); O2(0.253,0.0,0.502)
$P2_12_12_1$-B_2O_3	46	6.067	$a = 4.149$ Å, $b = 7.377$ Å, $c = 3.965$ Å	B1 (0.922,0.827,0.881); B2 (0.078,0.995,0.407) O1 (0.588, 0.835, 0.996); O2 (0.403, 0.022, 0.541); O3 (0.066, 0.346, 0.962)
$Pmmn$-B_2O_3	133	4.860	$a = 6.703$ Å, $b = 6.369$ Å, $c = 2.277$ Å	B1 (0.5, 0.385, 0.0); B2 (0.177, 0.264, 0.5) B3 (0.0, 0.995, 0.0); O1 (0.5, 0.621, 0.0) O2 (0.5, 0.119, 0.0); O3 (0.346, 0.376,0.5); O4 (0.668, 0.869, 0.5)
$C2/m$-B_2O_3	179	4.484	$a = 9.422$ Å, $b = 2.242$ Å, $c = 4.358$ Å $\beta = 103^\circ$	B1 (0.662, 0.0, 0.304); B2 (0.916, 0.0, 0.208) O1 (0.0, 0.5, 0.253); O2 (0.671, 0.5, 0.574) O3 (0.833, 0.0, 0.908)

and crystalline B_2O_3 [38]. Wu *et al.* [37] observed $^{[4]}$B in aluminoborosilicate glass at about 0.5 GPa, while Solozhenko *et al.* [38] recently reported the transition from B_2O_3-I to B_2O_3-II at 2 GPa and 600 K.

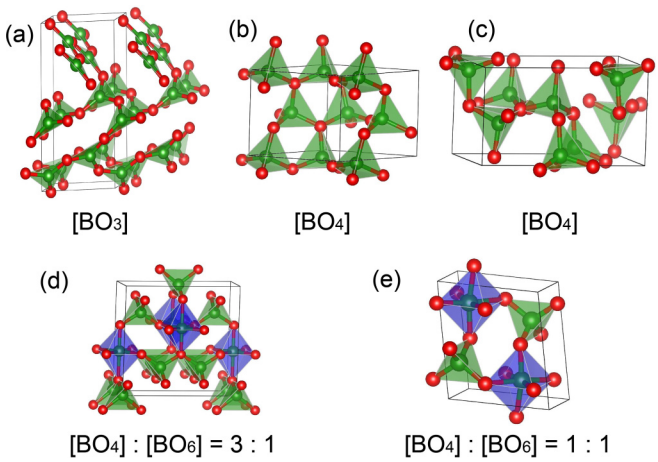

FIG. 3. Crystal structures of (a) $P3_121$-B_2O_3, (b) $Cmc2_1$-B_2O_3, (c) $P2_12_12_1$-B_2O_3, (d) $Pmmn$-B_2O_3, and (e) $C2/m$-B_2O_3. [BO_4] : [BO_6] = 3 : 1 indicates the ratio of [BO_4] and [BO_6] polyhedra is 3:1 in the structure.

From 46 to 133 GPa, a previously unknown crystalline phase, $P2_12_12_1$-B_2O_3, is predicted to be stable. Its structure is made of BO_4 tetrahedra, just like $Cmc2_1$-B_2O_3; see Fig. 3(c). Between 133 and 179 GPa, another unique structure, $Pmmn$-B_2O_3, is stable. Its structure contains both BO_4 tetrahedra and BO_6 octahedra. At higher pressures, above 179 GPa, $C2/m$-B_2O_3 is stable—and here, we again find both BO_4 tetrahedra and BO_6 octahedra. In addition, we also found an interesting phenomenon: The BO_4 tetrahedra and the BO_6 octahedra in $C2/m$-B_2O_3 disappear and convert into BO_3 units when pressure is released down to 0 GPa, as shown in Fig. S3 (Supplemental Material [31]). This is in contrast with $Cmc2_1$-B_2O_3 and $P2_12_12_1$-B_2O_3, which maintain their structure with BO_4 tetrahedra on decompression down to ambient pressure (where they are dynamically stable). The latter two phases may retain their original symmetry and dense structural topology under ambient pressure. $Cmc2_1$-B_2O_3 has for a long time been known to be quenchable in experiment [6], which is in good agreement with our prediction. The computed hardnesses of $Cmc2_1$- and $P2_12_12_1$-phases of B_2O_3 at zero pressure are 35 and 33 GPa from the Chen-Niu model (or 34 and 29 GPa from the Lyakhov-Oganov model) (Table II). Moreover, both structures are dynamically and mechanically stable at ambient pressure (Fig. S4 in the Supplemental Material [31] and Table II). This means that these

TABLE II. Elastic constants, bulk and shear moduli, and hardnesses of B_6O and B_2O_3 at ambient pressure, in GPa. *Pmmn* and $C2/m$ phases of B_2O_3 are mechanically unstable at ambient pressure.

Crystal	B_6O $R\bar{3}m$	B_6O $Cmcm$	B_2O_3-I $P3_121$	B_2O_3-II $Cmc2_1$	B_2O_3 $P2_12_12_1$	B_2O_3 $Pmmn$	B_2O_3 $C2/m$
c_{11}	585	584	175	352	461	376	573
c_{22}		441		354	323	22	6
c_{33}	458	563	66	468	396	678	6
c_{44}	178	192	57	148	153	−22	3
c_{55}		209		149	117	−587	10
c_{66}		197	66	173	170	26	1
c_{12}	124	75	43	78	73	16	2
c_{13}	50	90	10	40	48	−33	2
c_{14}	23		18				−2
c_{15}							8
c_{23}		66		40	24	3	3
c_{46}							−0.3
G (V-R-H)[a]	208	209	55	158	155	19	21
B (V-R-H)[a]	227	226	53	164	161	69	35
B (expt.)	228[b]		18.4[c]	169.9[d]			
Hv (Chen)	38[e]	39[e]	19	35	33		
Hv (Lyakhov)	32[e]	32[e]	32	34	29		
Hv (expt.)	33–36[f]		1.5 ± 5[g]	16 ± 5[g]			

[a]These were calculated from the elastic constants and Voigt-Reuss-Hill averaging was used [41].
[b]Reference [42].
[c]Reference [33].
[d]Reference [32].
[e]Reference [12].
[f]Reference [40].
[g]Experimental report of hardness of glass-like B_2O_3 (the local structure of glass-like B_2O_3 is closest to the structure of B_2O_3-I) and β-B_2O_3 (i.e., B_2O_3-II), Ref. [43].

two phases can be synthesized at high pressure (e.g., 5 and 50 GPa for $Cmc2_1$-B_2O_3 and $P2_12_12_1$-B_2O_3, respectively, with diamond-anvil cells or even a multianvil apparatus) and then may be decompressed to ambient pressure. They may be superior to B_6O, since B_6O is usually somewhat oxygen-deficient B_6O_x, where $x < 0.9$, and has rather poor crystallinity [39]. Moreover, even though B_6O, when prepared under high pressure, has excellent hardness, its fracture toughness is rather low [40].

For B_2O_3-I, both elastic moduli and hardness are overestimated (Table II), because B_2O_3-I has an exotic layered-like structure, as shown in Fig. 3(a), with folded layers bridged by B-O bonds. Such a delicate structure is a difficult case for theory, largely because of the importance of van der Waals interactions, and we see a large difference between theoretical and experimental bulk moduli (Table II). For the other B-O phases, e.g., $Cmc2_1$-B_2O_3 and $P2_12_12_1$-B_2O_3, as shown in Figs. 3(b) and 3(c), the situation is different. For example, the bulk modulus of $Cmc2_1$-B_2O_3 calculated by Voigt-Reuss-Hill theroy (164 GPa) is in good agreement with the experimental result (169.9 GPa; see Table II) [32]. The empirical Chen-Niu model is presently the most accurate model of hardness and has scored excellent successes, correctly reproducing experimentally measured hardnesses of many materials [28]. Therefore, the moduli and hardness of $Cmc2_1$-B_2O_3 and $P2_12_12_1$-B_2O_3 predicted by these empirical models are credible.

Glasses with high hardness have been in demand for many years. B_2O_3 is one of the most common glass materials and the hardness of $Cmc2_1$-B_2O_3 and $P2_12_12_1$-B_2O_3 crystals is much higher than that of the known oxide glasses. It may be possible to increase the fraction of local environments similar to $Cmc2_1$-B_2O_3 or even $P2_12_12_1$-B_2O_3 in the glass and enhance the hardness of the glass by applying pressure in the process of glass production.

High-pressure-temperature techniques are very important for the synthesis of novel materials. To further study the high-pressure synthesis conditions, the pressure-temperature phase diagram of B_2O_3 (Supplemental Material [31], Fig. S5) was constructed within the quasiharmonic approximation as implemented in the PHASEGO code [44] (considering only solid phases). At room temperature, $P3_121$-B_2O_3 transforms into $Cmc2_1$-B_2O_3 at 2.9 GPa, which is consistent with experiment [38], and $Cmc2_1$-B_2O_3 transforms into $P2_12_12_1$-B_2O_3 at 43 GPa and 300 K.

We analyze the relationship between the volume V, density ρ, average B-O bond length, coordination number of boron, charge transfer, and band gap as a function of pressure, as shown in Fig. 4. Volume and density as a function of pressure are shown in Figs. 4(a) and 4(b); one can see a series of volume discontinuities corresponding to first-order phase transitions. Bond lengths decrease with pressure for a given crystal structure—but at phase transitions involving increase of coordination number they sharply increase, resulting in a sawtooth-like dependence, and keeping roughly the same average B-O bond length, in the range 1.37–1.46 Å, in the enormous pressure range 0–500 GPa. At the same

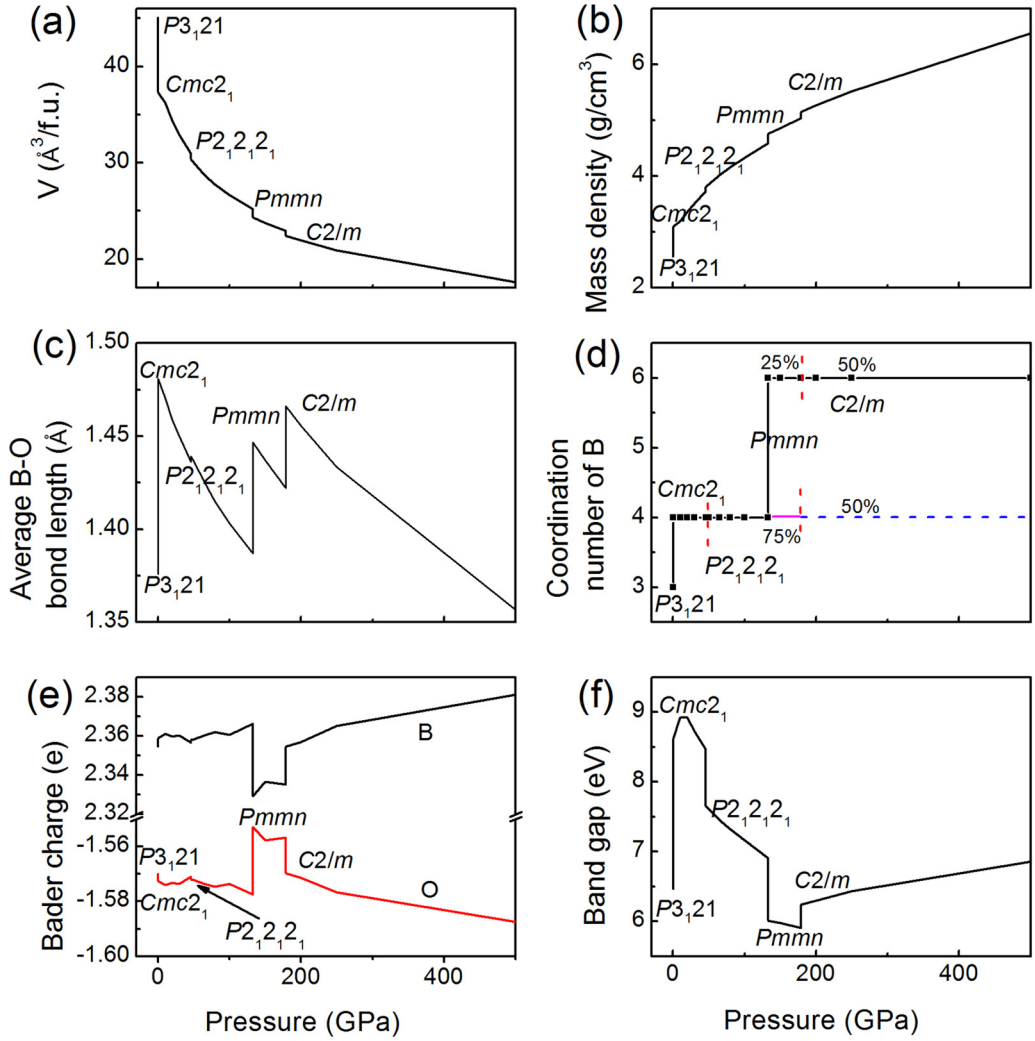

FIG. 4. Volume V, density ρ, average B-O bond length, coordination number (C-N) of boron atoms, Bader charges, and the DFT band gap as a function of pressure in B_2O_3.

time, atomic charges seem to be not sensitive to structural transitions [Fig. 4(e)]. The DFT band gap [Fig. 4(f)] shows large variations with pressure; the largest values roughly correspond to structures with tetrahedral coordination of boron atoms. For most phases, we see the normal tendency for the band gap to decrease with pressure, but notably, the band gap of $C2/m$-B_2O_3 increases with the increase of pressure from 179 GPa to at least 500 GPa.

In the sequence of phase transitions of B_2O_3, i.e., $P3_121$-$B_2O_3 \rightarrow Cmc2_1$-$B_2O_3 \rightarrow P2_12_12_1$-$B_2O_3 \rightarrow Pmmn$-$B_2O_3 \rightarrow C2/m$-$B_2O_3$, there is a monotonic increase of the coordination number of boron atoms ($^{[3]}B \rightarrow {}^{[4]}B \rightarrow {}^{[6]}B$), corresponding to the evolution $BO_3 \rightarrow BO_4 \rightarrow BO_6$ of boron coordination polyhedra. Fivefold coordination $^{[5]}B$ is not found in any of the stable phases.

IV. SUMMARY

To summarize, we have searched systematically for stable compounds in the B-O system in the pressure range 0–500 GPa using the *ab initio* evolutionary algorithm USPEX. We found that there are only two thermodynamically stable oxides, B_6O and B_2O_3. None of the previously discussed B_2O, B_7O, $B_{13}O_2$, or $B_{22}O$ are thermodynamically stable. Calculations reveal a theoretical ground state of superhard B_6O at ambient conditions and three hitherto unknown stable high-pressure phases of B_2O_3. Importantly, both of them are dynamically and mechanically stable at ambient pressure. Therefore, it is possible to synthesize them at high pressure and quench to ambient pressure: Synthesis of $Cmc2_1$-B_2O_3 and $P2_12_12_1$-B_2O_3 requires pressures in the ranges 0.5–46 and 46–133 GPa, respectively (at zero Kelvin). A 6×8 double stage multianvil press with sintered diamond cubes as the second stage can generate pressure up to ~50 GPa, with sample volumes ~1 mm^3, suitable for synthesis of these phases, with hardness reaching 34 GPa; these phases are harder than stishovite (32 GPa) and represent the hardest known proper oxides (B_6O suboxide is basically a boron-based insertion compound). Finally, we find that the sequence of coordination number changes of boron atoms in B_2O_3 under pressure is $^{[3]}B \rightarrow {}^{[4]}B \rightarrow {}^{[6]}B$.

ACKNOWLEDGMENTS

H.D. and Q.W. gratefully acknowledge financial support from the National Natural Science Foundation of China

(Grants No. 11604056 and No. 11504004) and the Natural Science Foundation of Guangdong, China Funds for Distinguished Young Scholar (Grants No. 2017B030306003 and No. 2016A030310352). X.Z. thanks the National Science Foundation of China (Grants No. 11674176 and No. 11874224) and the Tianjin Science Foundation for Distinguished Young Scholars (Grant No. 17JCJQJC44400). V.V.B. is grateful to the Russian Science Foundation for the financial support (Project No. 14-22-00093). A.R.O. acknowledges funding from the Russian Science Foundation (Grant No. 16-13-10459). H.D. expresses thanks for funding from the China Scholarship Council (ID No. 201708440119).

[1] A. R. Oganov, J. Chen, C. Gatti, Y. Ma, Y. Ma, C. W. Glass, Z. Liu, T. Yu, O. O. Kurakevych, and V. L. Solozhenko, Nature **457**, 863 (2009).
[2] Q. An, K. M. Reddy, K. Y. Xie, K. J. Hemker, and W. A. Goddard, Phys. Rev. Lett. **117**, 085501 (2016).
[3] A. J. Mannix, X. F. Zhou, B. Kiraly, J. D. Wood, D. Alducin, B. D. Myers, X. Liu, B. L. Fisher, U. Santiago, J. R. Guest *et al.*, Science **350**, 1513 (2015).
[4] B. J. Feng, J. Zhang, Q. Zhong, W. B. Li, S. Li, H. Li, P. Cheng, S. Meng, L. Chen, and K. H. Wu, Nat. Chem. **8**, 564 (2016).
[5] G. E. Gurr, P. W. Montgomery, C. D. Knutson, and B. T. Gorres, Acta Crystallogr. B **26**, 906 (1970).
[6] C. T. Prewitt and R. D. Shannon, Acta Crystallogr. B **B24**, 869 (1968).
[7] T. Edwards, T. Endo, J. H. Walton, and S. Sen, Science **345**, 1027 (2014).
[8] V. V. Brazhkin, Y. Katayama, K. Trachenko, O. B. Tsiok, A. G. Lyapin, E. Artacho, M. Dove, G. Ferlat, Y. Inamura, and H. Saito, Phys. Rev. Lett. **101**, 035702 (2008).
[9] K. Trachenko, V. V. Brazhkin, G. Ferlat, M. T. Dove, and E. Artacho, Phys. Rev. B **78**, 172102 (2008).
[10] A. Vegiri and E. I. Kamitsos, Phys. Rev. B **82**, 054114 (2010).
[11] H. T. Hall and L. A. Compton, Inorg. Chem. **4**, 1213 (1965).
[12] H. Dong, A. R. Oganov, Q. Wang, S.-N. Wang, Z. Wang, J. Zhang, M. Mahdi Davari Esfahani, X.-F. Zhou, F. Wu, and Q. Zhu, Sci. Rep. **6**, 31288 (2016).
[13] A. Kharlamov and N. Kirillova, Powder Metall. Met. C+ **41**, 97 (2002).
[14] C. E. Holcombe and O. J. Horne, J. Am. Ceram. Soc. **55**, 106 (1972).
[15] A. R. Badzian, Appl. Phys. Lett. **53**, 2495 (1988).
[16] Q. Li, W. Chen, Y. Xia, Y. Liu, H. Wang, H. Wang, and Y. Ma, Diamond Relat. Mater. **20**, 501 (2011).
[17] H. Hubert, L. A. J. Garvie, K. Leinenweber, P. R. Buseck, W. T. Petuskey, and P. F. McMillan, in *Materials Research Society Symposium—Proceedings*, edited by R. Bormann, G. Mazzone, R. D. Shull, R. S. Averback, and R. F. Ziolo (Materials Research Society, Warrendale, PA, 1995), Vol. 410.
[18] H. Hubert, B. Devouard, L. A. J. Garvie, M. O'Keeffe, P. R. Buseck, W. T. Petuskey, and P. F. McMillan, Nature **391**, 376 (1998).
[19] F. P. Bundy, H. T. Hall, H. M. Strong, and R. H. Wentorf, Nature **176**, 51 (1955).
[20] R. H. Wentorf Jr., J. Chem. Phys. **26**, 956 (1957).
[21] A. R. Oganov and C. W. Glass, J. Chem. Phys. **124**, 244704 (2006).
[22] A. R. Oganov, A. O. Lyakhov, and M. Valle, Acc. Chem. Res. **44**, 227 (2011).
[23] A. O. Lyakhov, A. R. Oganov, H. T. Stokes, and Q. Zhu, Comput. Phys. Commun. **184**, 1172 (2013).
[24] J. P. Perdew, K. Burke, and M. Ernzerhof, Phys. Rev. Lett. **77**, 3865 (1996).
[25] G. Kresse and J. Furthmüller, Comput. Mater. Sci. **6**, 15 (1996).
[26] P. E. Blöchl, Phys. Rev. B **50**, 17953 (1994).
[27] A. Togo, F. Oba, and I. Tanaka, Phys. Rev. B **78**, 134106 (2008).
[28] X.-Q. Chen, H. Niu, D. Li, and Y. Li, Intermetallics **19**, 1275 (2011).
[29] A. O. Lyakhov and A. R. Oganov, Phys. Rev. B **84**, 092103 (2011).
[30] S. Grimme, J. Comput. Chem. **27**, 1787 (2006).
[31] See Supplemental Material at http://link.aps.org/supplemental/10.1103/PhysRevB.98.174109 for the stability and the structural information of the predicted structures.
[32] D. Nieto-Sanz, P. Loubeyre, W. Crichton, and M. Mezouar, Phys. Rev. B **70**, 214108 (2004).
[33] V. L. Solozhenko, O. O. Kurakevych, V. Z. Turkevich, and D. V. Turkevich, J. Phys. Chem. B **112**, 6683 (2008).
[34] Q. An, K. M. Reddy, H. Dong, M.-W. Chen, A. R. Oganov, and W. A. Goddard, Nano Lett. **16**, 4236 (2016).
[35] H. Effenberger, C. L. Lengauer, and E. Parthe, Monatsh. Chem. **132**, 1515 (2001).
[36] F. Claeyssens, J. N. Hart, N. C. Norman, and N. L. Allan, Adv. Funct. Mater. **23**, 5887 (2013).
[37] J. Wu, J. Deubener, J. F. Stebbins, L. Grygarova, H. Behrens, L. Wondraczek, and Y. Yue, J. Chem. Phys. **131**, 104504 (2009).
[38] V. L. Solozhenko, O. O. Kurakevych, Y. Le Godec, and V. V. Brazhkin, J. Phys. Chem. C **119**, 20600 (2015).
[39] T. Lundström, J. Solid State Chem. **133**, 88 (1997).
[40] M. Herrmann, I. Sigalas, M. Thiele, M. M. Müller, H. J. Kleebe, and A. Michaelis, Int. J. Refract. Met. Hard Mater. **39**, 53 (2013).
[41] R. Hill, Proc. Phys. Soc., London, Sect. A **65**, 349 (1952).
[42] M. C. Tushishvili, C. V. Tsagareishvili, and D. S. Tsagareishvili, J. Hard Mater. **3**, 225 (1992).
[43] V. A. Mukhanov, O. O. Kurakevich, and V. L. Solozhenko, J. Superhard Mater. **30**, 71 (2008).
[44] Z. L. Liu, Comput. Phys. Commun. **191**, 150 (2015).